

Influence of Vacuum Heat Treatment on the Residual Stress of Thermal Spray Cermet Coatings

R. Ahmed *, H. Yu, L. Edwards, and J. R. Santisteban

Abstract— The aim of this investigation was to ascertain the changes in residual stress profile after the post-treatment of functionally graded thermal spray WC-NiCrBSi coatings, and relate these changes to the microstructural transformations. Through thickness residual stress measurements were performed using the neutron diffraction and x-ray diffraction techniques. Functionally graded HVOF (JP5000) WC-NiCrBSi coatings were thermally sprayed on AISI 440C steel substrate discs. These coatings were then heat-treated in an inert atmosphere at 1200°C for one hour. Microstructural investigations using SEM, XRD, and light microscopy were used to identify the changes after the heat-treatment. Microhardness and indentation modulus values were also investigated to analyse the changes in the mechanical properties after the heat-treatment. Results of this investigation indicated that the residual stress gradient within the coating material decreases after the heat-treatment, and the stress field in the substrate, near the coating substrate interface, changes from tensile to compressive. Residual stress measurements via x-ray diffraction provided average compressive values which were similar to those evaluated via the neutron diffraction technique, however the definition of stress gradient as a function of coating thickness was much better resolved via the neutron diffraction technique. The changes in the stress gradient after the heat-treatment were related to the microstructural changes which resulted in the formation of diffusion zones at the coating substrate interface, and also at the interface of functionally graded coating, improvement in coating elasticity due to the changes in the bonding mechanism from mechanical interlock to metallurgical bonding, and the formation of secondary phases within the coating microstructure.

Index Terms— Heat-treatment, Neutron diffraction, Residual stress, Thermal spray coating, X-ray diffraction.

I. INTRODUCTION

Thermal spraying is a molten or semi-molten state process in which the coating material is heated and accelerated towards the substrate to form a coating. Innovative advances in thermal

spraying technology have led their use in numerous applications including aerospace, automotive, metal/paper rolling, oil drilling, construction, marine, and biomedical industries [1]-[4]. The increasing number of applications is at least partly due to the improved microstructure offered by the advanced coating systems, such as High Velocity Oxy-Fuel (HVOF), Low Pressure Plasma Spraying (LPPS), and emerging technologies such as the use of hybrid laser systems and High-Density Infrared (HDI) technology [2], [3]. Excellent corrosive, erosive, and abrasive wear resistance of these coatings e.g. WC-Co, WC-Co-Cr has resulted in environmentally friendly solutions to engineering problems, including improved efficiency, longer life, and salvaging of worn/undersized/over-machined components to meet dimensional requirements [2], [4].

Despite these improvements, microstructural defects within the coating however lower the cohesive and adhesive strength, leading to fracture and spalling. A major factor influencing the spalling and delamination resistance of thermal spray coatings is the residual stress profile within the coating and substrate material. The generics of thermal spraying process induce complex residual stress fields made up of combinations of the quenching (micro-tensile) residual stresses produced at the splat level due to the very high cooling rates (e.g. 1000 K/ms for Ni) of individual lamellae, and the macro-compressive or tensile residual stresses due to the mismatch of the coefficient of thermal expansion of the coating and substrate materials [5].

Post-treatment of thermal spray coatings has been shown to refine the microstructure e.g. by eliminating porosity and microcracks, and to promote beneficial phase transformations and metallurgical bonding within the coating microstructure [6], [7]. However, studies relating to the relative changes in the residual stress profile due to post treatment have been very limited. This is due to the fact that although experimental techniques such as deep hole drilling, x-ray diffraction, and changes in curvature have all long been applied to measure the residual stress profile in thermal spray coatings, the methodology of these measurements makes them destructive for the WC-cermet coatings. Even in the case of conventional x-ray and high-energy synchrotron diffraction techniques, the low penetration depth of x-rays in WC-cermets makes layer removal compulsory for depth profiling of residual stress field. Such techniques can therefore not be directly applied for through thickness non-destructive stress or strain profiling of finished components. Due to the difficulties in the non-destructive residual stress profiling of these coatings, there

Manuscript submitted March 20, 2007.

*R. Ahmed is with School of Engineering and Physical Sciences, Heriot-Watt University, Edinburgh, EH14 4AS, UK (corresponding author, e-mail: R.Ahmed@hw.ac.uk; phone: +44(0)1314514722).

H. Yu is with School of Engineering and Physical Sciences, Heriot-Watt University, Edinburgh, EH14 4AS, UK.

L. Edwards is with Department of Materials Engineering, The Open University, Walton Hall, Milton Keynes, MK7 6AA, UK

J. R. Santisteban is with Rutherford Appleton Laboratory, ISIS, Didcot, OX11 0QX, UK.

have recently been a limited number of investigations [8], [9], where neutron-diffraction technique, due to its high penetration depth, have been successfully applied to non-destructively measure residual stresses profile in thicker (typically 1000 μm thick) Thermal Barrier Coatings (TBC's) of Zirconia, NiCrAlY and Ytria Stabilized Zirconia. These investigations have provided valuable information about the stress gradients, theoretical modelling of stress generation and their influence on coating performance of relatively thicker thermal spray coatings. However studies related to relatively thinner (100 to 300 μm) thermal spray coatings are very limited. It is therefore the aim of this investigation to compare the residual stress profile after the post-treatment of relatively thinner thermal spray cermet coatings via neutron diffraction and x-ray diffraction techniques, and relate these changes to the microstructural transformations occurring during the post-treatment.

II. EXPERIMENTAL TEST PROCEDURE

A. Coating Preparation

Thermal spray coatings were functionally graded to avoid the mismatch of mechanical and thermal properties at the coating substrate interface. Two compositions of the spray dried and sintered WC-NiCrBSiFeC composite powders i.e. 10 wt.% Ni alloy - 90 wt.% WC, and 40 wt.% Ni alloy - 60 wt.% WC were used in this investigation. The substrates were AISI 440C stainless steel discs of 31 mm diameter and 8 mm thickness. HVOF JP-5000 spraying was carried out using the parameters summarised in Table I. The first layer of WC-40%wtNiCrBSiFeC was deposited onto the substrate to an approximate thickness of 100 μm , and then the second layer of WC-10%wtNiCrSiFeBC was subsequently applied to achieve a total as-sprayed coating thickness of approximately 500 μm . Coatings were then ground and polished to achieve an average total thickness of 400 μm .

Table I – Spraying parameters

Spray gun	JP-5000
Oxygen flow	8931 lit/min
Kerosene flow	0.321 lit/min
Spraying distance	380 mm
Spraying rate	50 g/min

B. Coating Post-treatment

The heat-treatment of un-encapsulated coatings was carried out in an argon environment to prevent the oxidation of the coated specimens. The coated discs were placed in the furnace, which was evacuated of air, filled with argon and heated at $4^\circ\text{C}\cdot\text{min}^{-1}$ to a temperature of 1200°C . The coatings were held for 1hr at 1200°C , before being cooled at a rate of $4^\circ\text{C}\cdot\text{min}^{-1}$ until 800°C , and then allowed to cool to room temperature outside the furnace.

C. Powder and Coating Characterisation

The x-ray diffraction (XRD) analysis was carried out using a Siemens D500 diffractometer with Cu-K α radiations (x-ray wavelength = 1.5406 \AA , step size of 0.02° , and dwell time of 2

s). The spray powders and the coatings were also characterised using a scanning electron microscope utilising secondary electron and energy-dispersive x-ray detectors. Microhardness measurements were carried out under a load of 2.94 N using a Vickers microhardness (Mitutoyo-Mvk-H1) test machine.

Elastic modulus measurements were also performed via the indentation method [10]. The indentation modulus (Y_{HV}) was measured using the real time displacement of the force indentation curve during the hardness tests, which were carried out under a load of 500 mN, and correlated to the Young's modulus (E) and Poisson's ratio (ν) using the following equation.

$$E = Y_{HV} (1 - \nu^2) \quad (1)$$

D. Residual Stress Measurements via Neutron Diffraction

Neutron diffraction measurements were performed at ISIS (Rutherford Laboratory, UK), using a dedicated strain measurement diffractometer (ENGIN-X) [11]. This is a pulsed neutron diffractometer equipped with slits and collimators to achieve small gauge volumes. This instrument operates in a fundamentally different manner from most reactor-based instruments, as instead of measuring Bragg reflections by scanning a detector from low to high 2θ , ENGIN-X uses a pulsed polychromatic beam to measure Bragg reflections at a fixed scattering angle ($2\theta = 90^\circ$) using the time of flight of each diffracted neutron to characterise its wavelength [12].

The "vertical scan" configuration of stress measurement was adapted in the current investigation as shown schematically in Fig. 1. Details of the vertical scanning arrangement can be seen in Ahmed et al. [13]. In this arrangement the coated specimen was moved up or down in the z-direction for depth profiling of strain in the coating and substrate materials. The incident beam was passed through a vertical and horizontal slit assembly to give a beam height at the slits of 0.5 mm. However due to beam divergence (Penumbra effects), the actual gauge volume was 1 mm \times 1 mm \times 10 mm. The technique of partially submerged gauge volume was adapted to measure the strain in the coated material, whereas most of the substrate strain was measured using a fully submerged gauge volume. Longer measurement times were therefore required for strain measurement in the coating material. The centre of gravity of the gauge volume was used to measure the depth of strain measurement. Strain measurement analysis of the diffracted beams was based upon the shift in individual WC (101) and Fe (alpha or gamma) peaks for the coating and substrate materials, respectively, obtained via the Pawley refinement technique.

The strain free lattice parameter (d_0) for the coating material was obtained by carefully removing the coating from the substrate and crushing the deposit to form a powder. This powder was then put in a vanadium tube and its diffraction was measured using a neutron beam of dimensions 4 mm \times 4 mm \times 4 mm. Although a straightforward measurement of the starting powder used for thermal spraying would have been easier, this technique was adapted to avoid any changes in the lattice parameters due to metallurgical changes during the thermal spraying process. The strain free lattice parameter for the steel substrate was measured at the near-surface of the substrate disc.

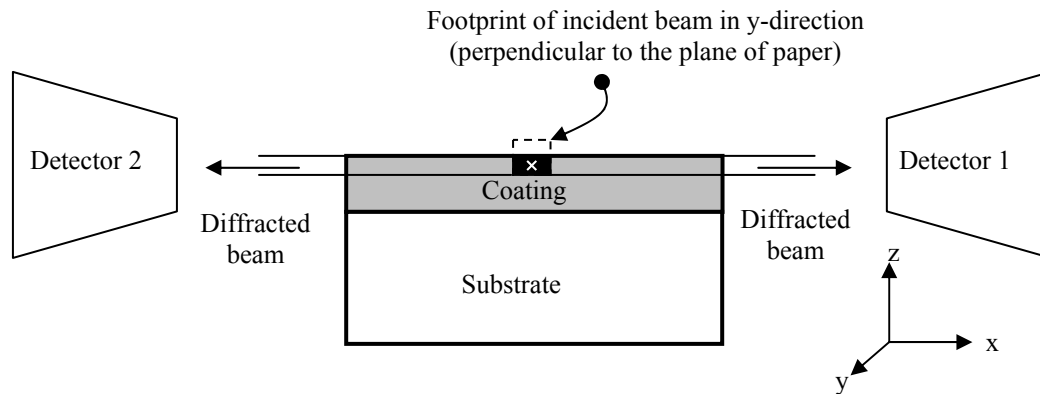


Fig. 1 Vertical (z) scan configuration for in-plane strain used for neutron diffraction measurements (diffraction angle 2θ is fixed at 90° for both detectors). Cross indicates the centre of gravity of partially submerged gauge volume.

Residual strain (ε) values were calculated using the shift in the diffraction peak using the equation:

$$\varepsilon = \frac{d - d_0}{d_0} \quad (2)$$

where d and d_0 were the measured and strain-free lattice parameters, respectively. Residual strain values were then related to the residual stress values using the modulus data by using (1).

E. Residual Stress Measurements via X-ray Diffraction

The residual stress in the coatings via x-ray diffraction was measured using the $\sin^2\psi$ technique, which relies on the slope of the 2θ vs. $\sin^2\psi$ plot for stress measurement [14]. A RIGAKU-RINT 2000 diffractometer with Cr-K α source was used for these measurements at the voltage and current settings of 40 kV and 200 mA, respectively. Eight ψ angles between 0 and 36° were used for the stress measurements. Due to the low penetration depth of x-rays in WC-cermet, 20 μm layers of the coating material were electropolished for depth profiling of the residual stress in the coating material. No correction was applied to account for the changes in the lattice parameters due to coating removal. Further details of the experimental methodology can be seen elsewhere [15].

III. EXPERIMENTAL RESULTS AND DISCUSSION

A. Microstructural Identifications

Scanning electron micrographs of the as-sprayed and heat-treated coatings are presented in Figs. 2 and 3. These figures show the main features of the two coatings, highlighting the difference between them at higher magnifications. Fig. 2a shows the overall view of the coating cross-section, indicating the deposition of the WC-40%NiCrBSi, and WC-10%NiCrBSi layers. The higher magnification image at the interface of the two coating layers (Fig. 2b) indicate lamella structure, which is typical of the thermal spray coating process. The XRD evaluations of these coatings are summarised in Fig. 4. These results indicate that some WC transformed to W_2C . Furthermore, the broadening of the XRD peak at approximately 40 degrees indicate some amorphous (nanocrystalline) phase, which resulted from the rapid solidification of the impacting lamella. These changes are typical of the decomposition of

WC-cermet coatings which occur from two different sources as summarised by Lovelock [16] and Verdon et al. [17]. Firstly, the loss of carbon in the form of CO_2 due to the combustion of oxygen in the HVOF flame, and secondly the formation of amorphous/nano-crystalline phases through WC solubility in the matrix, which results in nano-crystalline binder phase due to the rapid cooling during coating deposition. These two mechanisms led to the decomposition of WC into W, W_2C and formation of amorphous regions around 2θ of approximately 40 degrees.

The microstructural transformations occurring during the heat-treatment (Figs. 3 and 4) indicate diffusion of elemental species between the top/bottom coating layers, and also at the coating substrate interface. These changes resulted in the formation of two distinct diffusion zones at these interfaces, as identified in Figs. 3a and 3c. Higher magnification investigations of the diffusion zone indicated that there was some carbide dissolution near the coating substrate interface. In addition to the formation of these diffusion zones, Kirkendall voids were also observed in the coating microstructure. This was based on unequal diffusion between the bottom coating layer and substrate, causing an excess of vacancies, which ultimately become pores (Kirkendall pores). The XRD results indicate formation of additional carbide and secondary phases (FeW_3C , Cr_7C_3 , Cr_{23}C_6 , NiB_2 , Ni_4B_3). The nano-crystalline phase observed in the as-sprayed coatings also crystallised after the heat-treatment, as identified by a sharp diffraction peak around 2θ of approximately 40 degrees. These phase changes resulted in an increase in the hardness and elastic modulus after the heat-treatment.

B. Microhardness and Indentation Modulus Measurements

The results of microhardness and indentation modulus measurements are summarised in Fig. 5. The hardness values for the as-sprayed coatings varied between 1000 and 1160 HV, which is typical of the WC-cermet coatings [1]. The average substrate hardness before the heat-treatment was 270 HV. After the heat-treatment, coating's hardness increased substantially to a range of 1200 to 1500 HV for the top coating layer, whereas the hardness decreased to an approximate value of 900 HV for the lower coating layer. In addition, the hardness of the substrate increased to approximately 640 HV. The increase in coating hardness was associated with the formation of

secondary phase carbides in the microstructure (FeW_3C , Cr_7C_3 , Cr_{23}C_6), whereas the softening of the lower coating layer was associated with the formation of two diffusion zones, i.e. one above and the other below it (Fig. 3), which also resulted in some carbide dissolution in the lower coating layer.

The indentation modulus results of the as-sprayed coatings indicated an average value of coatings Young's modulus of 200 GPa, which can be evaluated for a typical Poisson's ratio of 0.25 for the coating material (2). This is consistent with the elastic modulus values of WC-cermet thermal spray coatings in the published literature [1], [18]. During the heat-treatment, the intersplat bonding changed from the mechanical interlock, which is the main bonding mechanism in the as-sprayed coatings, to metallurgical bonding caused by the diffusion of elemental species in the coating microstructure. Hence much higher values of elastic modulus were observed after the heat-treatment (Fig. 5). The improvement in the bonding mechanism varied almost linearly throughout the coating thickness, with the maximum value at the coating surface, where the modulus increased to almost 500 GPa, which is similar to the modulus of sintered WC. The change in the modulus of the second coating layer was marginal, indicating that the carbide dissolution associated with the diffusion zone compromised the advantage of metallurgical bonding in the bottom coating layer.

C. Residual Stress Measurements via Neutron and X-ray Diffraction

Fig. 6 summarises the residual stress measurement results obtained using the neutron diffraction technique. Neutron diffraction analysis results indicate that the coating and substrate stress varies significantly with the heat-treatment. These results indicate that the stress in both coating materials was compressive, which was mainly due to the higher value of the coefficient of thermal expansion of the substrate material. The residual stress value in the substrate was therefore tensile in the as-sprayed coatings, whereas it varied from compressive to tensile within the substrate of the heat-treated coating.

The neutron diffraction analysis results also indicated that the compressive stress values in the as-sprayed coating varied between 54 to 1053 MPa, whereas these values varied between 262 and 722 MPa for the heat-treated coating. The average values of stress in the as-sprayed and heat-treated coating layers can be approximated as 553 and 492 MPa, respectively. The residual stress gradient in the heat-treated coating was less steep, which should be beneficial during the mechanical loading of the component to resist crack propagation. These differences in the residual stress profile were a result of the formation of diffusion zones (Fig. 3), which reduced the stress gradient after the post-treatment, and the improvement of bonding mechanism from mechanical interlock to metallurgical bonding as observed in the indentation modulus measurements.

The residual stress values measured via x-ray diffraction in the top coating layer are shown in Fig. 7. The results of these measurements also indicate compressive stress values, with an average of 785 ± 40 MPa and 815 ± 60 MPa for the as-sprayed and HIPed coatings, respectively. These average compressive stress values are higher than the average values obtained via the neutron diffraction technique, although the difference in

average values is not significant. The results obtained via the x-ray diffraction analysis were however unable to highlight the differences of stress variation through coating thickness in the as-sprayed or heat-treated conditions. There are two main reasons for this behaviour, which relate to the measurement technique. Firstly, no correction factor was applied to account for the changes in the stress distribution due to the removal of electro-polished layer. Secondly, due to the very low penetration depth of x-rays in dense WC-cermet, which is typically around 2 to 5 μm , the gauge volume for x-ray diffraction include a significant proportion of layer influenced by the layer removal method. Both of these factors have less significant influence in relatively low density materials where the penetration depth of x-rays is of the order of tens of micrometers. However in the case of WC-cermet, the introduction of layer removal can significantly influence the through thickness stress measurement.

Albeit this drawback, x-ray diffraction is useful in predicting near-surface residual stress changes in WC-cermet in cases such as sliding wear, since changes relating to wear mechanisms such as material shakedown, abrasion, ploughing, etc. are related to very near surface residual stress changes. However, the through thickness variation of residual stress can not only be measured non-destructively using the neutron diffraction analysis, but also the variation of the stress field can be resolved to much higher definition, improving the accuracy of the residual stress results for the subsequent design and modelling process. Resistance to the spalling and delamination of thermal spray coatings, either from within the coating microstructure or at the coating substrate interface, can therefore be improved by the detailed information of the through thickness residual profile, and incorporating a designed residual stress profile during the post-treatment process.

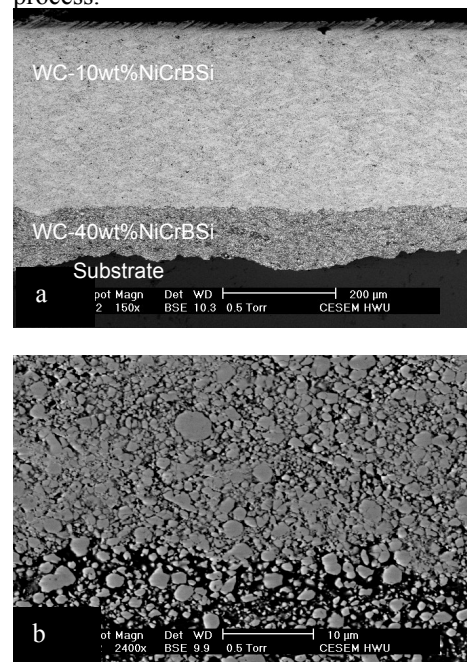


Fig. 2 SEM observations of the as-sprayed coating; a) overall view of as-sprayed coating, b) higher magnification image of the interface of two coating layers.

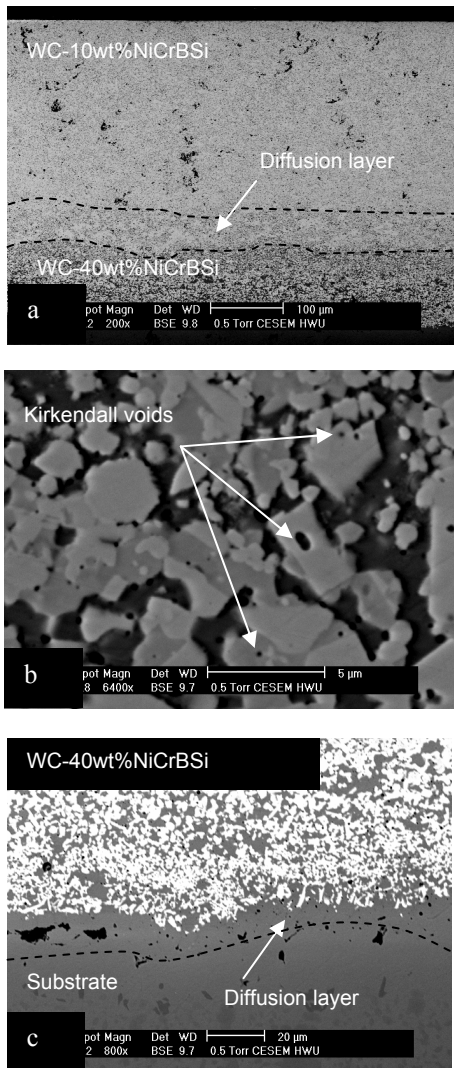


Fig. 3 SEM observations of the heat-treated coating; a) heat-treated coating indicating diffusion layer at the interface of two coating layers, b) heat-treated coating indicating sintering of carbides in the bottom coating layer, c) coating substrate interface indicating diffusion layer.

IV. CONCLUSIONS

1. Residual stress measurements via neutron diffraction analysis indicate an attenuation of stress gradient within the coating layer after the heat-treatment. The changes in the stress field are associated with the formation of diffusion zones, and changes in the bonding mechanisms from mechanical interlock to metallurgical bonding within the coating microstructure.
2. The residual stress results via x-ray diffraction analysis although provide an average measure of the compressive stress within the coating material, the variation of stress field through the coating thickness is much better resolved via the neutron diffraction technique.
3. Inter-splat bonding improves after the coating post-treatment which was reflected by the changes in coating elasticity.
4. Microstructural investigations indicate phase transformations within the coating layers and at the

substrate interface after the heat-treatment, resulting in secondary carbides and solid solution strengthening, increasing the average hardness of the coating and substrate materials.

ACKNOWLEDGMENT

Authors would like to acknowledge the support of ISIS (Grant number RB15141) for neutron diffraction measurements. They would like to thank Dr Susan Davies at Bodycote HIP Ltd., UK for her support during the HIPing post-treatment of coatings, and Prof. S. Tobe of Ashikaga Institute, Japan for x-ray diffraction analysis.

REFERENCES

- [1] L. Pawlowski, *The Science and Engineering of Thermal Spray Coatings*, Wiley, 1995.
- [2] R. L. Daniel, H. L. Sanders, M. J. Mendrek, "Replacement of environmentally hazardous corrosion protection paints on the space shuttle main engine using wire arc sprayed aluminium", *Proceedings of National Thermal Spray Conference*, Boston, USA, 1994, pp. 93-98.
- [3] T. Miyamoto, and, S. Sugimoto, "Current conditions and future trends of thermal spray technology in the Japanese automobile industry", *Proceedings of International Thermal Spray Conference*, Kobe, Japan, 1995, pp. 3-8.
- [4] H. Chen, I. M. Hutchings, "Abrasive wear resistance of plasma-sprayed tungsten carbide cobalt coatings", *Surface & coatings technology*, vol. 107 (2-3), 1998, pp. 106-114.
- [5] S. C. Gill, *Residual Stress in Plasma Sprayed Deposits*, PhD Thesis, Gonville and Caius college, Cambridge University, UK, 1993.
- [6] P. K. Ghosh, Ram, & Neki, "Characteristics of heat treated tungsten carbide embedded nickel base hard surfacing on structural steel produced by gas thermal spray process", *Int. Journal of Joining Materials*, vol. 9(3), 1997, pp. 114-121.
- [7] K. A. Khor, N. L. Loh, "Hot isostatic pressing of plasma sprayed Ni-base alloys", *Journal of thermal spraying*, vol. 3(1), 1994, pp. 57-62.
- [8] J. Matejicek, S. Sampath, P. C. Brand, H. J. Prask, "Quenching, thermal and residual stress in plasma sprayed deposits: NiCrAlY and YSZ coatings", *Acta Mater.*, vol 47(2), 1999, pp. 607-617.
- [9] S. Sampath, X. Y. Jiang, J. Matejicek, L. Prchlik, A. Kulkarni, A. Viadya, "Role of thermal spray processing method on the microstructure, residual stress and properties of coatings: an integrated study for Ni-5wt.%Al bond coats", *Mat. Sci. Eng. A*, vol. 364, 2004, pp. 216-231.
- [10] M. Buchmann, M. Escribano, R. Gadow, G. Burkle, "On the elastic mechanical properties of thermally sprayed coatings", *Thermal Spray: Surface Engineering via Applied Research*, C. C. Berndt, Ed, ASM International, 2002, pp. 598-605.
- [11] J. A. Dann, M. R. Daymond, L. Edwards L, J. A. James, and J. R. Santisteban, "ENGIN-X: First results from a new diffractometer optimised for stress measurement", *Physica B: Condensed Matter*, vol. 350, 2004, pp. E511-E514.
- [12] M. W. Johnson, L. Edwards, and P. J. Withers, "ENGIN - A new instrument for engineers", *Physica B*, vol. 234, 1997, pp.1141-1143.
- [13] R. Ahmed, H. Yu, S. Stewart, L. Edwards and J. Santisteban, "Residual strain measurement in thermal spray cermet coatings via neutron diffraction", *ASME journal of Tribology*, vol. 129(2), 2007, pp. 411-418.
- [14] B. D. Cullity and S. R. Stock, *Elements of X-Ray Diffraction*, Prentice-Hall, 2001.
- [15] R. Ahmed and M. Hadfield, "Experimental measurement of the residual stress field within thermally sprayed rolling elements", *Wear*, vol. 209, 1997, pp. 84-95.
- [16] H. L. Lovelock, "Powder/processing/structure relationships in WC-Co thermal spray coatings: A review of the published literature", *Journal of thermal spray technology*, vol. 7(3), 1998, pp. 357-373.
- [17] C. Verdon, A. Karimi, J. L. Martin, "A study of high velocity oxy-fuel thermally sprayed tungsten carbide coatings. Part I: Microstructures", *Materials Science and Engineering-A*, vol. A246, 1998, pp. 11-24.

[18] H. Nakahira, K. Miyajima, Y. Harada, "Anisotropy of thermally sprayed coatings", *Proc. ITSC, Thermal Spray Coatings: Research Design and Applications*, Orlando, USA, 1992, pp. 1011-1017.

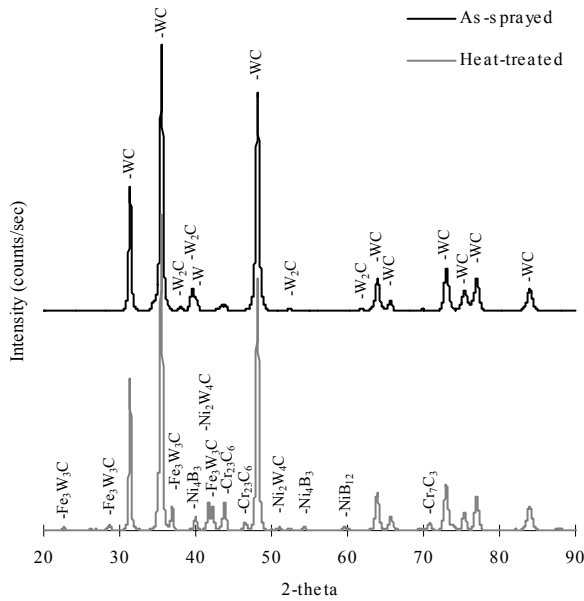


Fig. 4 XRD results of the top coating layer for the as-sprayed and heat-treated coatings.

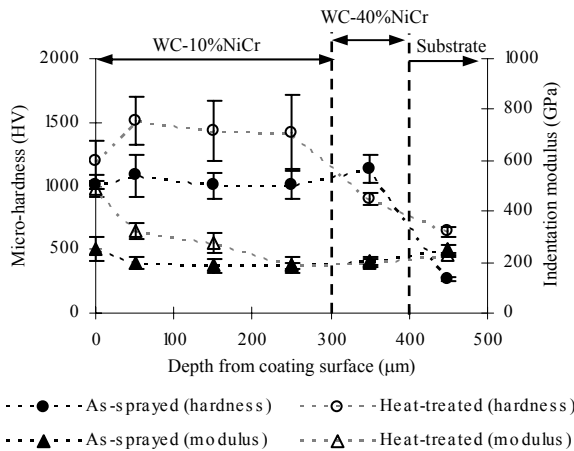


Fig. 5 Microhardness and indentation modulus results for the as-sprayed and heat-treated coatings.

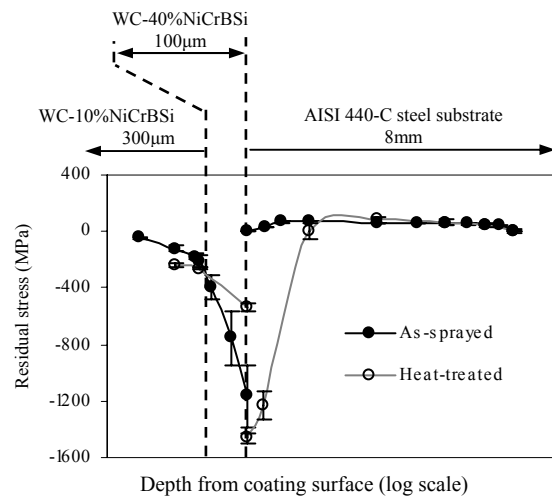


Fig. 6 Through thickness residual stress profile via neutron diffraction technique.

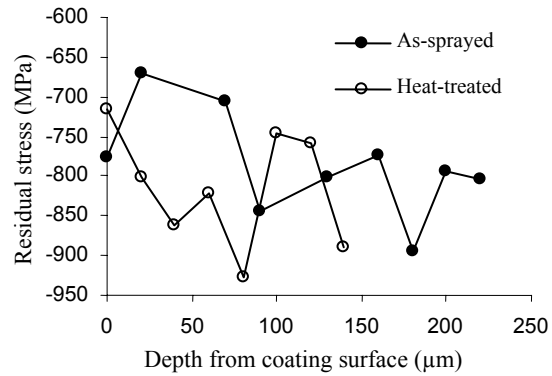


Fig. 7 Through thickness residual stress profile in top coating layer via x-ray diffraction technique.